




Article

Research on the Tribological Properties of a New Generation of Multi-Layer Nanostructured PVD Coatings for Increasing the Technological Lifetime of Moulds

Janette Brezinová ^{1,*} , Miroslav Džupon ², Viktor Puchý ² , Jakub Brezina ³, Pavlo Maruschak ⁴ , Anna Guzanová ³ , Lýdia Sobotová ⁵ and Miroslav Badida ⁵

¹ Department of Automotive Production, Faculty of Mechanical Engineering, Technical University of Kosice, Letná 9, 042 00 Košice, Slovakia

² Institute of Materials Research, Slovak Academy of Sciences, Watsonova 47, 040 01 Košice, Slovakia; mdzupon@saske.sk (M.D.); vpuchy@saske.sk (V.P.)

³ Department of Technology, Materials and Computer Supported Production, Faculty of Mechanical Engineering, Technical University of Kosice, Letná 9, 042 00 Košice, Slovakia; jakub.brezina@tuke.sk (J.B.); anna.guzanova@tuke.sk (A.G.)

⁴ Department of Industrial Automation, Ternopil Ivan Puluj National Technical University, Ruska Str. 56, 46001 Ternopil, Ukraine; maruschak.tu.edu@gmail.com

⁵ Department of Business Management and Environmental Engineering, Faculty of Mechanical Engineering, Technical University of Kosice, Letná 9, 042 00 Košice, Slovakia; lydia.sobotova@tuke.sk (L.S.); miroslav.badida@tuke.sk (M.B.)

* Correspondence: janette.brezinova@tuke.sk

Abstract: This paper presents the results of research focused on increasing the lifespan of HPDC moulds for casting aluminium alloys by applying duplex PVD coatings in combination with laser texturing the base material before the coatings' deposition. This article describes the HPDC process and the degradation mechanisms of the moulds that arose during this process. The PVD nanostructured coatings utilised, the methods of their deposition, and the evaluation of their wear resistance are defined in this paper. The surface texturing process is described alongside the description of the analysis of the wear of the functional parts of the mould after decommissioning, which was carried out by visual inspection and optical and light microscopy. Three types of PVD duplex coatings were analysed during our study. The coatings were deposited using the LARC technology method (lateral rotating cathode). Subsequently, the procedure of laser texturing in the form of dimple textures using a laser was proposed. The quality of the coatings was evaluated under tribological conditions by means of the "Ball on disc" method. Based on the experimental results, recommendations for practice are established.

Keywords: high-pressure casting; release agent; PVD coatings; texturing; adhesion; COF



Citation: Brezinová, J.; Džupon, M.; Puchý, V.; Brezina, J.; Maruschak, P.; Guzanová, A.; Sobotová, L.; Badida, M. Research on the Tribological Properties of a New Generation of Multi-Layer Nanostructured PVD Coatings for Increasing the Technological Lifetime of Moulds. *Metals* **2024**, *14*, 131. <https://doi.org/10.3390/met14010131>

Academic Editor: Jianqiang Wang

Received: 8 December 2023

Revised: 12 January 2024

Accepted: 17 January 2024

Published: 22 January 2024



Copyright: © 2024 by the authors. Licensee MDPI, Basel, Switzerland. This article is an open access article distributed under the terms and conditions of the Creative Commons Attribution (CC BY) license (<https://creativecommons.org/licenses/by/4.0/>).

1. Introduction

Aluminium alloy castings made with HPDC technology (high-pressure die casting) have found implementation in many fields of industry, but the automotive industry is their major customer. HPDC is a reliable technology that has the potential, under certain conditions, to produce large batches of products with repeatable and reproducible quality. The prerequisite is to continuously monitor the condition of the injection mould, which is subject to complex wear processes as the number of castings increases. The dominant wear mechanisms of mould parts and cores are the following: thermomechanical cyclic loading [1], dissolution of mould metal in aluminium [2,3], mechanical adhesive erosive cavitation wear, chemical soldering [4], aluminium buildup on mould wall, thermal fatigue, etc. [5,6].

Dadic [7] identified mould temperature and the impact speed of molten Al as the most critical factors. He found that preheating the mould to at least 200 °C (or, even better, to

270 °C) significantly reduces wear progression, while, on the contrary, a high impact speed of molten Al increases the wear. It would be ideal to keep the impact speed of molten aluminium at around 6 m/s, but this could slow down the mould duty cycle (stroke) and jeopardize the planned production volume. The same author identified the critical areas of a mould to be the sharp edges of the mould parts and the areas opposite to the melt inlet, where there is perpendicular contact of the pressurised melt flow with the surface. The dissolution of the mould material by the aluminium melt leads to the formation of buildup containing intermetallic phases, which makes it difficult to remove the casting from the mould or remove the cores from the casting when opening the mould [4]. The effect of core surface roughness and casting temperature on melt sticking and, hence, on the force required to remove the core from the casting was studied by Bai [8]. He found that the least sticking (soldering) occurs at the lowest core surface roughness and the lowest-allowable melt temperature. An increase in melt temperature leads to a coarsening of the carbides in the core's surface layer, which leads to a decrease in hardness and, hence, wear resistance of the surface heat-affected region of the core. Liu [9], in turn, experimented with thermal fatigue, looking for the relation between the cooling cycle and the resistance of a material against thermal fatigue and thermal cracking. He supported his results by developing a simulation model of crack initiation and growth due to the thermal fatigue of the material.

In the case of the onset of wear in the most exposed parts of the moulds or cores, it is necessary to intervene so that the deteriorated condition of the mould is not reflected in the quality of the castings. This is most often achieved using cladding or glow-spraying technologies. Cladding is used to replenish the worn material, while, at the same time, the correct choice of additive material can increase the wear resistance of the refurbished mould or core surface locally, according to the prevailing wear mechanism. In order to achieve a surface layer with different properties to the base material, it is necessary to clad the original material using two or three layers, since the first layer shows a mixing with the BM (basic material) of about 50%, the second layer less so, and the third layer presents only the properties of the additive material [2]. Brezinova et al., in [1], experimented with two-layer plasma transferred arc (PTA) technology cladding but also with three-layer GTAW cladding or disk laser cladding, CMT cladding, MIG pulse, or TopTIG technology. Many of these technologies have a low heat input and are suitable for local repairs of small cross-sections on the mould or core. To monitor mould breakage by dissolution in aluminium melt, the above-mentioned authors [2,8] developed a test consisting of immersing the base material and clads in aluminium melt and then monitoring the formation of intermetallic phases at the interface with the melt.

Refurbished surfaces need to be treated and subsequently have their wear resistance increased via coating with PVD, PACVD, CVD, or hot thermal diffusion (HTD) processes. Hard inert coatings such as TiN, CrN, DLC, TiCN, VC, B₄C, CrC, AlN, Al₂O₃, TiAlN, AlCrN, Si₃N₄, and many others, used as monolayers or multi-layers, are designed to reduce the coefficient of friction (COF) as the melt flows into the mould, limiting soldering and the formation of IMCs. However, if the integrity of the coating is compromised, the melt will reach the base material, dissolve it, and, subsequently, the coating will detach from the surface (detachment) [6,10,11]. Neto, in [6], identified the conditions for selecting a mould coating to minimize mould damage as follows: a COF should be less than 0.40; the wear rate should be in the range of 10⁻⁸ mm³/N·m; and the ratio between the worn scar diameter on the ball Δd and the ball diameter D should not exceed a value of 0.22.

Nanostructured coatings are a new generation of coatings that excel in some specific properties compared to commonly used coatings. They consist of at least two separate phases with a nanocrystalline or amorphous structure, which is formed by the segregation of one phase at the grain boundaries of the other phase. This layer growth mechanism inhibits grain growth and promotes nanostructure formation. The unique functional properties of nanostructured coatings are a result of the boundary regions surrounding the individual grains, which are up to 10 nanometres in size.

To achieve the desired grain size and ensure the development of the segregation phase, the deposition process parameters—current, temperature of the base material, bias of the sample, low current density of the base material, and partial pressure of the reactive gas used—need to be optimized. Grain growth is most affected by the kinetic energy of impact particles over a very small area. The minimum surface mobility of the atoms required to form the crystalline phase and sufficient diffusion in the segregation system is ensured by ion bombardment. A critical factor in the deposition process is the temperature of the process. Exceeding the critical temperature will cause grain growth. The addition of one or more alloying elements to the base material has the same effect on the formation of the nanostructure phase as a low-energy bombardment [12].

Another step in increasing mould life is the use of a release agent, which prevents soldering, facilitates the extraction of the casting from the mould, and further reduces the COF. In order for the release agent to perform these functions, it must perfectly wet the mould surface (small wetting angle) [6] and be retained on the mould surface for a sufficiently long time. One of the new trends in this field is the micro spraying of mould parts with a mould release agent. Its main advantage is to increase the quality of the working environment. Texturization of the mould surface prior to coating, which can take the form of stochastic or defined craters, creates a micro-space on the surface to store a supply of lubricant for several casting cycles [13].

Surface texturing is the creation of a three-dimensional topography—ordered patterns of various shapes on the surface of materials—in order to improve some material properties, e.g., reduction in COF and improvement of the adhesion of the coating to the substrate in the deposition process. Surface texturing is most often made using laser beam (LBT) or electron beam technology (EBT) [14].

In LBT texturing, a focused pulsed laser beam melts a micro volume of substrate material, which is vaporized and removed from the surface using vapour pressure, creating a pit or groove, either disordered or in an ordered pattern. Texturing can also be used on moulds for high-pressure casting, where it provides improved adhesion of the protective PVD coating and, thus, resistance to oxidation at high temperatures, serves as a release agent reservoir, and offers many other improved properties that increase the life of the mould and its shaped parts [15].

The shape of the texture significantly affects the effectiveness of its friction reduction and other properties. A number of simulations and experiments were performed on texture surface shapes to study individual textures, including typical rectangular, circular, elliptical, triangular, and V-shaped textures [16,17].

Texture shapes affect the micro-hydrodynamic lubrication effect, which in turn affects the contact between two surfaces and the friction characteristics.

Chen et al. [18] tested the properties of different textures in terms of their tribological properties and found that two texture parameters, depth and diameter of the pits, have a great influence on the COF and wear resistance of the coating.

This paper presents the influence of the presence of PVD duplex coatings on the textured and non-textured surfaces of a mould material on the technological lifespan of the moulds for HPDC. The aim of surface topography modification by texturing and PVD coating will be to increase the technological durability of the mould shaped part of the mould for aluminium casting.

2. Experimental Aim and Method

The aim of this article is the preparation of a renovated mould for the HPDC of aluminium alloys with an improved surface by applying three types of PVD nanostructured coatings on a textured surface. The created texture, i.e., the pits, is intended to simultaneously serve as a reservoir for the separating agent during the casting process, allowing it to form a thermal barrier between the casting and the steel surface of the mould. A continuous layer of release agent is intended to reduce the friction of the high-speed flowing melt with the steel surface of the mould.

The goal of this research was to select the optimal PVD coating to use alongside laser texturing, which will increase the technological life of moulds.

The effect of texturing on the resulting values of various coating properties was investigated. The following methods were used:

- Evaluation of coating adhesion—scratch test method;
- Evaluation of COF coatings—ball-on-disc method.

Mould Wear Assessment Methodology

The evaluation of the intensity of mould wear was performed on the shaped parts of the movable part of the mould, which were discarded from production after 200,000 cycles, covered with molten aluminium alloy. The quality of the surface of the worn mould before renovation was checked with a visual inspection according to the standard STN EN 13018 [19]. During the casting cycle for the given mould, the parameters of high-pressure casting, listed in Table 1, were used; also, for the treatment of the shaped parts of the mould, a separating agent marked Safety Lube 7815 was used, which is a separating agent commercially used in practice.

Table 1. High-pressure die casting parameters.

High-Pressure Die Casting Parameters	
Impact area	225 mm ²
Piston speed	4 m·s ⁻¹
Velocity of the melt upon impact	100 m·s ⁻¹
Filling the mould cavity	3 s
Solidification period of the cast in the form	2 s
Total contact time of the casting with the mould cavity	14 s

Subsequently, samples were taken from the shaped parts of the movable part of the mould, without the thermal influence of the material for a material analysis and a mould wear analysis. The material analysis consisted of determining critical areas of the shaped parts of the mould using light and electron microscopy, followed by a chemical elemental EDX analysis of these areas in order to identify their individual phases. An OLYMPUS GX71 light microscope (Olympus Deutschland, GmbH, Hamburg, Germany) and observation in the bright field was used. A Jeol JSM 7000F scanning electron microscope (Jeol Ltd., Tokyo, Japan) with a THERMAL FEG auto-emission nozzle with the possibility of magnification up to 100,000 times was used for the EDX analysis. Microhardness measurements were performed in accordance with the standard STN EN ISO 6507-1 [20] with a Vickers indenter, a load of 4.903 N and dwell time of 15 s, using a WILSON-WOLPERT Tukon 1102 device (Buehler ITW Co., Ltd., Lake Bluff, IL, USA).

The base material for the experimental work was tool steel intended for high temperatures, Uddeholm Dievar (voestalpine High Performance Metals Deutschland GmbH, Düsseldorf, Germany), intended for the production of HPDC moulds, alloyed with Cr, Mo, V, and other alloying elements, produced by means of powder metallurgy. The chemical composition of the material is shown in Table 2, and its basic mechanical properties are shown in Table 3.

Table 2. Chemical composition of the basic material, Uddeholm Dievar.

Element	C	Si	Mn	Cr	Mo	V	Fe
wt. %	0.38	0.2	0.5	5	2.3	0.6	bal.

Table 3. Mechanical properties of the basic material, Uddeholm Dievar.

HRC	Rm [MPa]	Rp _{0.2} [MPa]	A [%]	Z [%]
44	1480	1210	13	55

For the needs of the experiment, two types of samples with non-textured and textured surfaces were created, where PVD duplex coatings were subsequently deposited on these surfaces.

For texturing, a Piranha Multi FL205-type laser device manufactured by ACSYS Lasertechnik (Kornwestheim, Germany) with a Yb fibre laser with a power of 20 W was used. Two types of pit textures were created: random and ordered. The use of a textured surface was meant to verify the assumption that the pits would act as reservoirs of separating agent to protect the mould and improve friction during individual HPDC cycles.

For the prepared non-textured as well as textured surfaces in cooperation with the company LISS s.r.o., three PVD duplex coatings were deposited:

- PVD duplex coating AlTiN G;
- PVD duplex coating AlXN₃;
- PVD duplex coating nACRo⁴.

AlTiN G is a high-performance gradient layer that is used to coat tools for machining materials with higher strength and hardness. The main area of application of this coating is the coating of drilling tools and the coating of moulds for high-pressure aluminium casting. AlXN₃ is a duplex coating where the first layer applied during the continuous duplex coating manufacturing process is a plasma-nitrided layer that improves the resulting adhesion of the coating to the substrate.

It is followed by PVD deposition of nano-multi-layer CrN–AlCrN coating, exhibiting some toughness, resulting in high abrasive wear resistance at elevated temperatures.

The coating nACRo⁴ is a nanocomposite coating of fourth generation characterised by sufficient toughness and abrasive wear resistance also at elevated temperatures. This nanocomposite is used to coat the tools for machining non-ferrous metals as well as HPDC moulds.

The final top layer is made of nc-AlCrN/a-Si₃N₄. For the coatings' deposition, the unique patented PLATIT LARC technology[®] (lateral arc cathode) was used: particularly, the PLATIT Pi411 equipment was used for the AlTiN G coatings' and AlXN₃ coatings' deposition, and a PLATIT Pi1511 device was used for the nACRo⁴ coatings' deposition.

The substrate roughness before the coatings' deposition recommended by the deposition company was 0.3 µm. The AlTiN G coating is a gradient, where two stages are indicated as follows:

- gradient 1—stage where the deposition starts;
- gradient 2—stage where the deposition ends.

The other coatings are multi-layers, where the deposition parameters of particular layers (layer 1 and layer 2) alternate, as shown in Table 4.

The micro-geometry of the surface with PVD nanostructured coatings as well as pit textures was observed using a ZEISS LSM 700 laser confocal microscope (Carl Zeiss Microscopy GmbH, Oberkochen, Germany). The surface roughness was assessed in accordance with the standard STN EN ISO 21920-2 [21].

The adhesion of the PVD coatings was measured with the scratch test method using a Bruker UMT 2 (Bruker Nano GmbH, Berlin, Germany) scratch tester with a Rockwell tip with a tip radius of 0.2 mm. The output of this test is the COF and the wear behaviour of surfaces in dry sliding conditions. Scratches with a length of 5 mm are made with a gradually increasing load up to 40 N at room temperature. The load at the first cohesive failure of the coating (Lc1) or the load at the adhesive failure of the coating (Lc2) is recorded when the coating has peeled off. In our experiment, the loading time was 70 s, and the speed of the indenter over the surface was 0.1 mm·s⁻¹. The length of the scratch was 7 mm.

After the scratch tests of the PVD duplex coatings, an EDX linear analysis of the post-test scratches was performed.

Table 4. Deposition parameters of PVD duplex coatings.

Coating	Apparatus	Deposition	I (A)	I (A)	I (A)	I (A)	Bias (V)	Temperature (°C)	Pressure (mbar)
AlTiN G	Pi 411	Gradient 1	Ti	Al	130	165	40	420	0.05
			105	155					
AlTiN G	Pi 411	Gradient 2	Ti	Al	105	155	40	420	0.05
			105	155					
AlXN ₃	Pi 411	Layer 1	Cr	Al	115	170	40	420	0.036
			115	170					
AlXN ₃	Pi 411	Layer 2	Cr	Al	90	175	30	420	0.032
			90	175					
nACRo ⁴	Pi 1511	Layer 1	Cr	AlSi	AlCr	AlCr	30	470	0.035
			200	160	65/35	65/35			
nACRo ⁴	Pi 1511	Layer 2	Cr	AlSi	AlCr	AlCr	60	470	0.032
			250	200	135	135			

The tribological properties of the PVD duplex coatings were evaluated under dry friction conditions with the ball-on-disc method using a universal tribometer BRUKER UMT 3 (Bruker Nano GmbH, Berlin, Germany) in accordance with the standard ASTM G133-05 [22]. The COF was determined for an untextured and textured surface with PVD duplex coatings, on which the Safety Lube 7815 release agent was applied. The Safety Lube 7815 release agent was applied by hand-spraying the PVD-coated samples, which had been applied to the untextured and textured surface of the substrate material. The samples were heated to 250 °C in a forced-atmosphere oven prior to the application of the Safety Lube 7815 release agent. This is the temperature to which the mould part is usually preheated for the HPDC of aluminium alloys. An SiC ball with a diameter of Ø 6 mm was used as the counterpart; the sliding distance was 500 m; the load was 5 N with a linear velocity of 0.10 m·s⁻¹. The mentioned procedure was designed to experimentally verify the suitability of the texturing of the surface with the aim of gradually releasing the separation agent from the pitted textures [23].

3. Results and Discussion

3.1. Analysis of Mould Wear

The mould was analysed after 200,000 casting cycles. Mechanical wear was detected after 200,000 cycles of high-pressure casting, at the point of contact between the moving core and the shaped part of the mould (Figure 1). In this contact, the surface of both parts delaminated, the so-called core and moving part of the mould, which caused peeling of the surface particles and led to a decrease in the technological life of the mould itself and its functional parts.

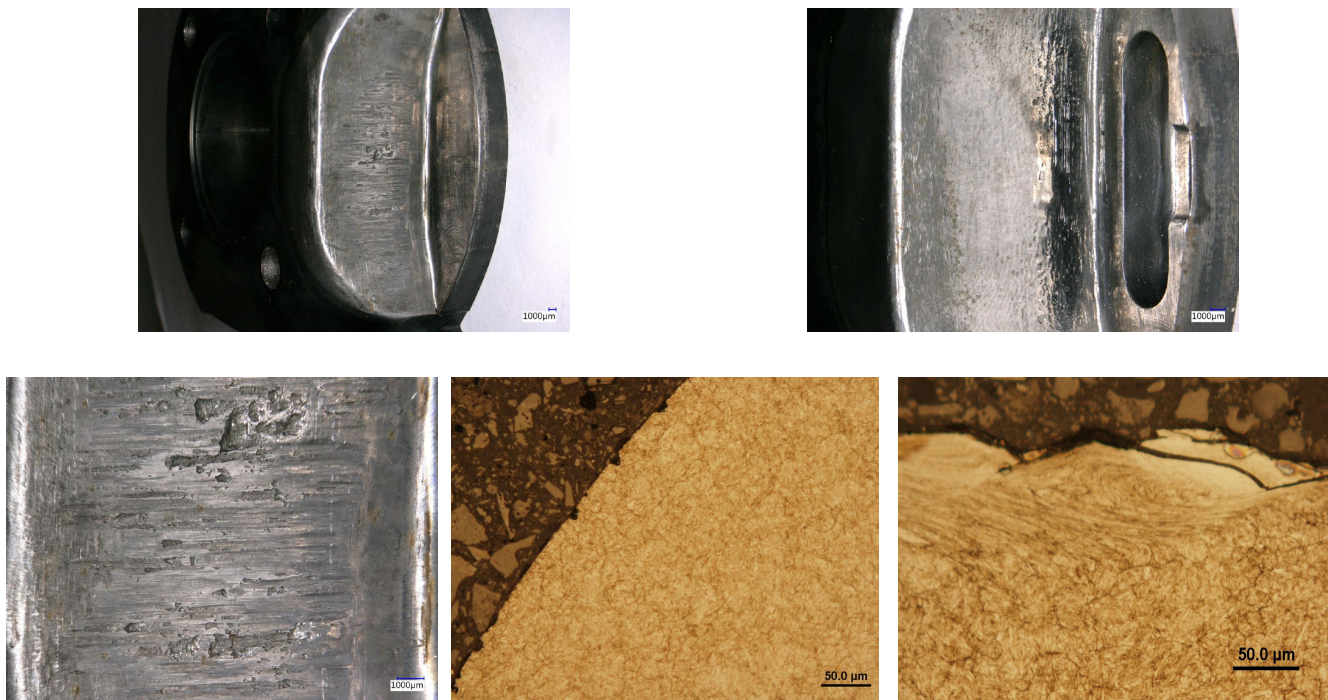


Figure 1. Mechanical wear of the shaped part of the mould and the movable core.

In the sharp corners and rounded transitions, wedge-shaped branched cracks in the microstructure of the shaped parts of the mould with a sharp tip at the root of the crack due to the repeated cycles of high-pressure casting were identified using light microscopy (Figure 2). Cracks were also observed around the ejector.

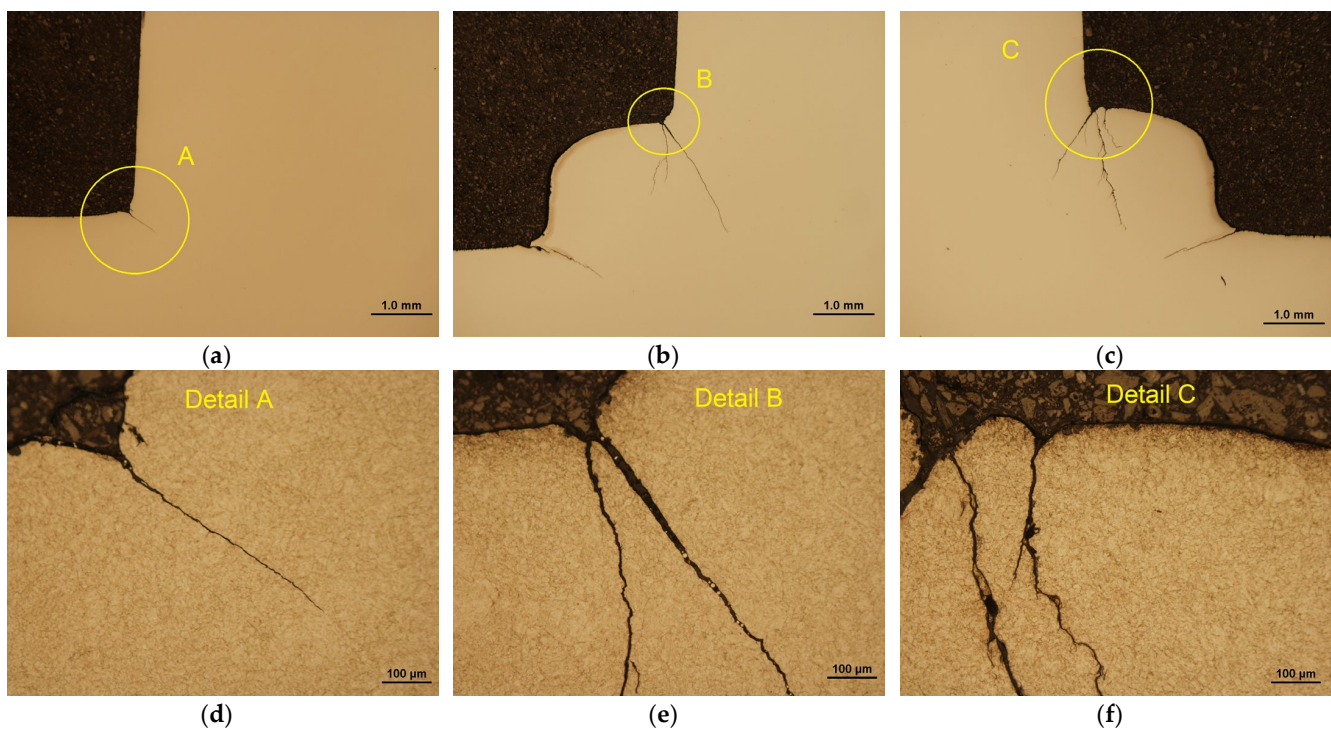


Figure 2. A few examples of branched wedge-shaped cracks in the sharp transitions of the mould taken at (a–c) low magnification, and in detail at high magnification (d–f).

3.2. Analysis of PVD Nanostructured Coatings

The duplex PVD coatings of AlTiN G with a 2 μm thickness, AlXN₃ with a 1 μm thickness, nACRO⁴ with a 4 μm thickness on the textured and substrate material were analysed using a semi-quantitative EDX microanalysis to determine the tentative chemical elemental composition of the coatings (Figure 3). The elements titanium, nitrogen, and aluminium were detected for the AlTiN G coating, while the elements chromium, nitrogen, aluminium, and silicon were detected for the AlXN₃ coating and the nACRO⁴ coating.

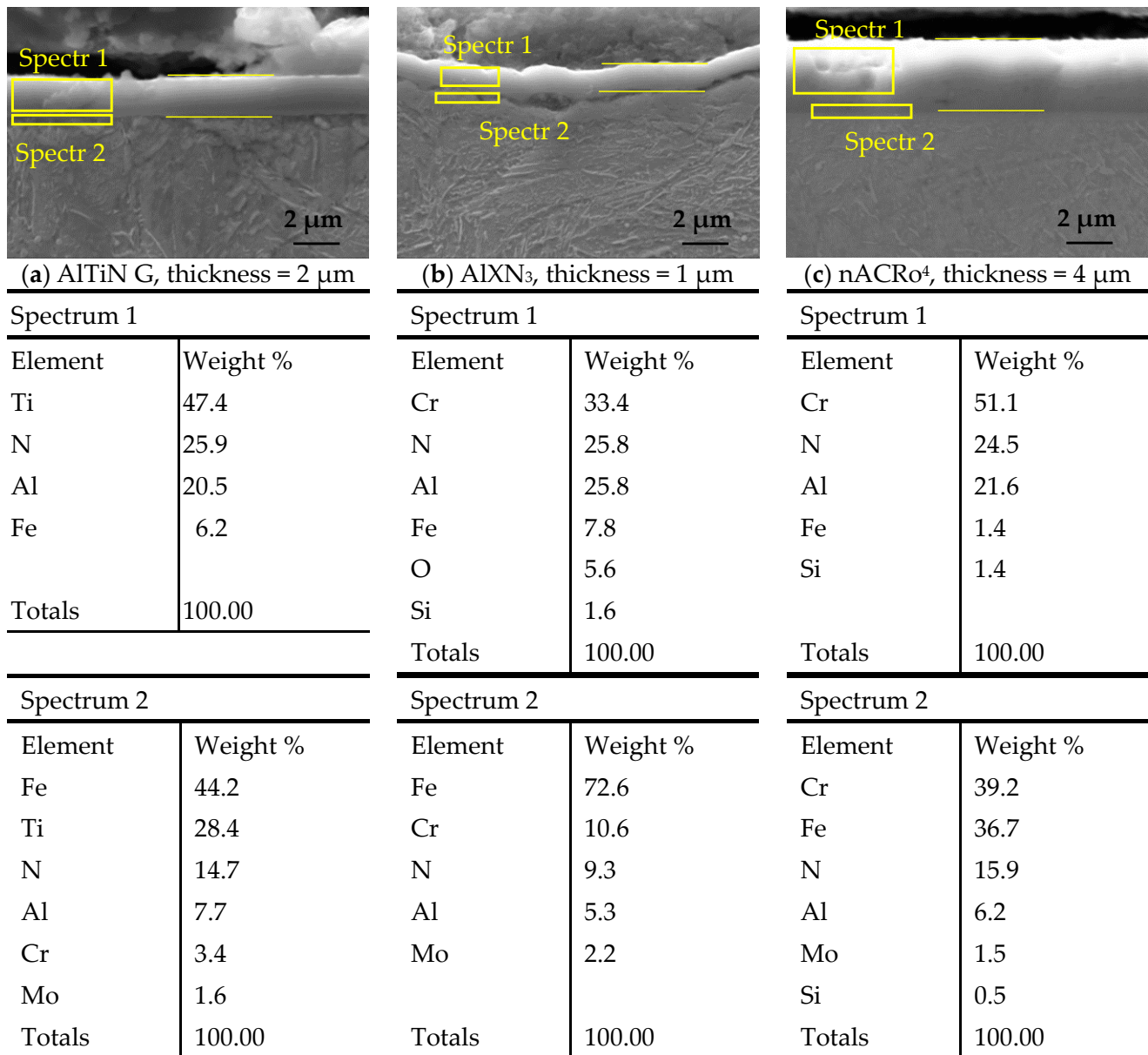
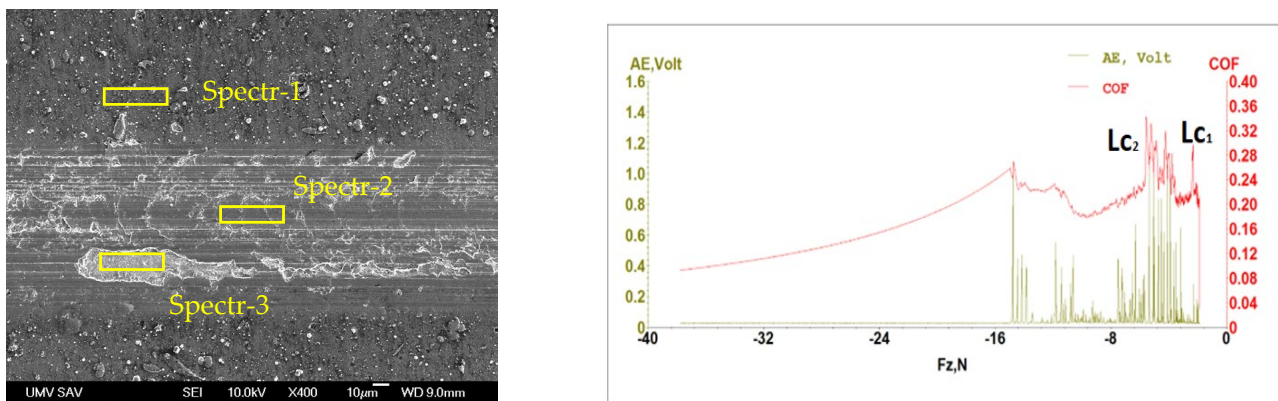


Figure 3. Cross-sections of the following coatings: (a) AlTiN G, (b) AlXN₃, and (c) nACRO⁴.

The scratch track on the AlTiN G coating observed using SEM is shown in Figure 4, together with COF and acoustic emission (AE) signal.



(a)			(b)					
Spectrum 1			Spectrum 2			Spectrum 3		
Element	Weight %	Atomic %	Element	Weight %	Atomic %	Element	Weight %	Atomic %
N K	31.39	53.12	N K	30.45	52.38	N K	1.82	6.66
Al K	33.71	29.61	Al K	32.38	28.92	Al K	0.83	1.57
Ti K	34.90	17.27	Ti K	37.17	18.70	Ti K	14.84	15.88
						Cr K	3.12	3.08
						Fe K	79.39	72.82
Totals	100.00		Totals	100.00		Totals	100.00	

(c)

Figure 4. Analysis of the scratch on the AlTiN G coating: (a) SEM image of a scratch track, (b) the course of the COF and AE, and (c) semi-quantitative EDX microanalysis of the track.

From Figure 4, it is clear that the first failure of the coating occurred in the first run-in phase at a value of 3.7 N. A complex failure of the coating was observed at 6 N at the end of the test, which was confirmed also by the AE signal. Cohesive failure in the form of semi-circular cracks of the AlTiN G coating in the entire track after the scratch test and adhesive failure in the form of peeled parts of the coating along the edges of the track were visible. The COF recorded during the test reached a maximum value of 0.34. Its course with fluctuations corresponds to the movement of the indenter on the roughened surface and the resistance of the tested material to further movement and penetration of the indenter. The COF is an accompanying value that is recorded during the scratch test. After the performed linear EDX SEM analysis, it was possible to state that, already in the first run-in phase of the scratch, when the indenter went up to the base material with almost 80 wt. % Fe, there was a perforation of the base material. The coating moved along the scratch path along with the steel material, which was evidenced by the higher proportion of Ti and Al.

Figure 5 shows results of scratch test on Al_xN₃ coating, i.e., SEM analysis of scratch track, COF and AE signal.

The critical failure loads and morphology of the prepared coatings were similar to those found by authors researching AlTiN-based coatings [24–26].

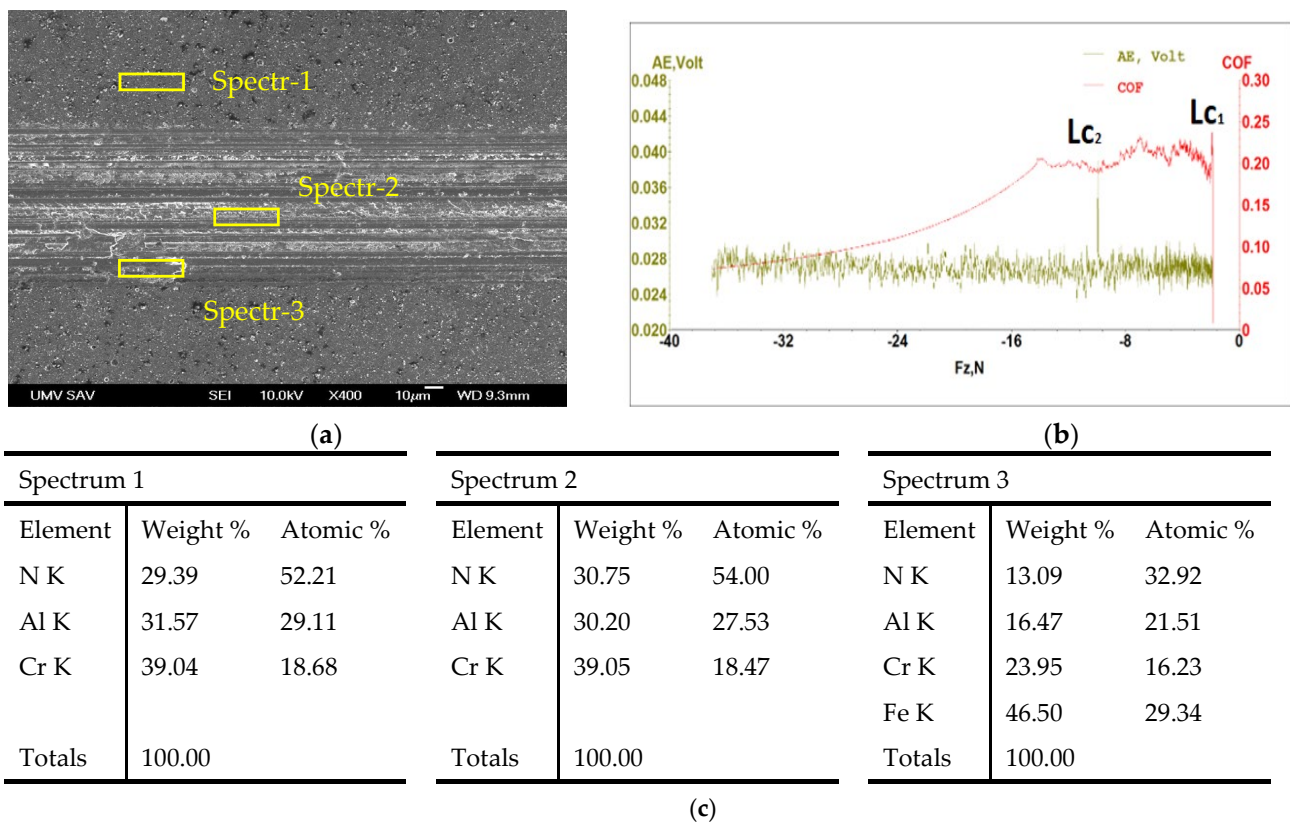


Figure 5. Analysis of the scratch on the AlCrN₃ coating: (a) SEM image of a scratch track, (b) the course of the COF and AE, and (c) semi-quantitative EDX microanalysis of the track.

Through the performed EDX SEM line analysis of the scratch with the AlCrN₃ (X = Cr) coating, a smaller proportion of iron was detected after the scratch test at the level of 4 wt. %. This confirms the fact that perforation of the evaluated coating did not occur and that the AlCrN₃ duplex coating had a satisfactory adhesion to the base material and showed better adhesion compared to the AlTiN G duplex coating, where a higher proportion of iron was measured already in the first run-in phase of the scratch test.

The morphology of the edge of the scratch was less rough, which can be attributed to the fact that the indenter went from the surface of the coating to its depth, but there was no damage to the base material found. For this reason, there was no mixing of the coating material and the steel material, nor was the material accumulated on the edges of the scratch. The mechanical and tribological properties of the AlCrN coating and of the AlCrN/FexN duplex coating deposited via PVD arc evaporation have been previously investigated by the author Ramírez-Reyna and his team [27]. They also investigated the effect of a nitriding pretreatment on the mentioned properties. In their study, the AlCrN coating was strongly separated at the edges of the wear track (rough peeling) due to its poor adhesion to the substrate. The damage changed from adhesive to cohesive. The AlCrN/FexN coating showed the lowest specific wear rate, and the damage severity was reduced. The AlCrN/FexN duplex coating showed the best results in terms of adhesion and wear resistance.

The SEM analysis of the scratch track on the duplex nACrO₄ coating is showed in Figure 6.

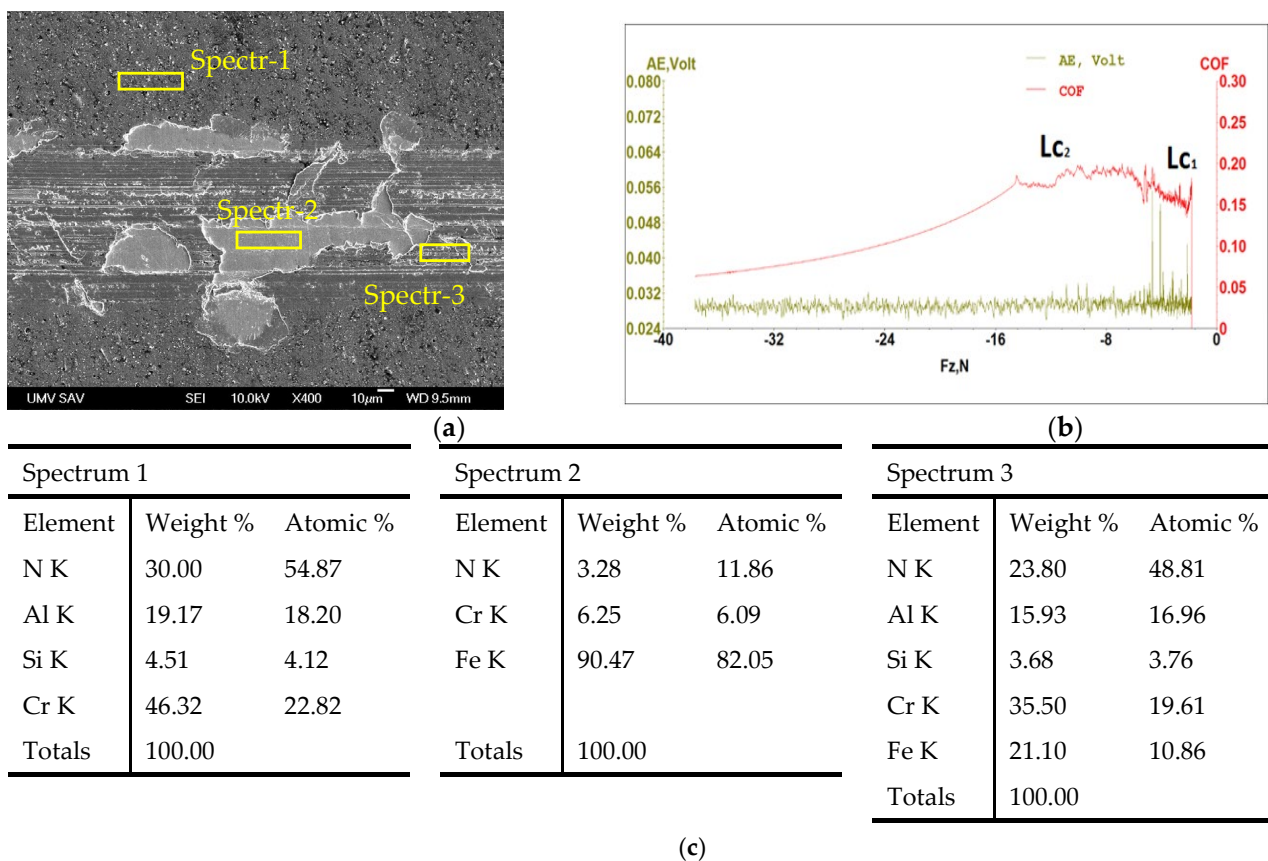


Figure 6. Analysis of the scratch on the nACrO₄ coating: (a) SEM image of a scratch track, (b) the course of the COF and AE, and (c) semi-quantitative EDX microanalysis of the track.

From the scratch test, it is clear that there was no cohesive failure, unlike what had been observed for the AlXN₃ coating. However, the adhesive failure of the coating was in the form of separated particles of coating transported towards the sides of the track. The first failure was recorded at 4.8 N; adhesive failure occurred at 14.7 N at the end of the test, confirmed also by an AE signal. The fluctuations in the COF were small; the indenter did not overcome such a high resistance. No significant roughening of the coating surface was observed. The sliding properties were even improved, which was reflected in the drop in the COF to a value of 0.15. The properties of the PVD coatings obtained in this study are comparable to those of similar materials reported in the literature [28].

3.3. Laser Surface Texturing

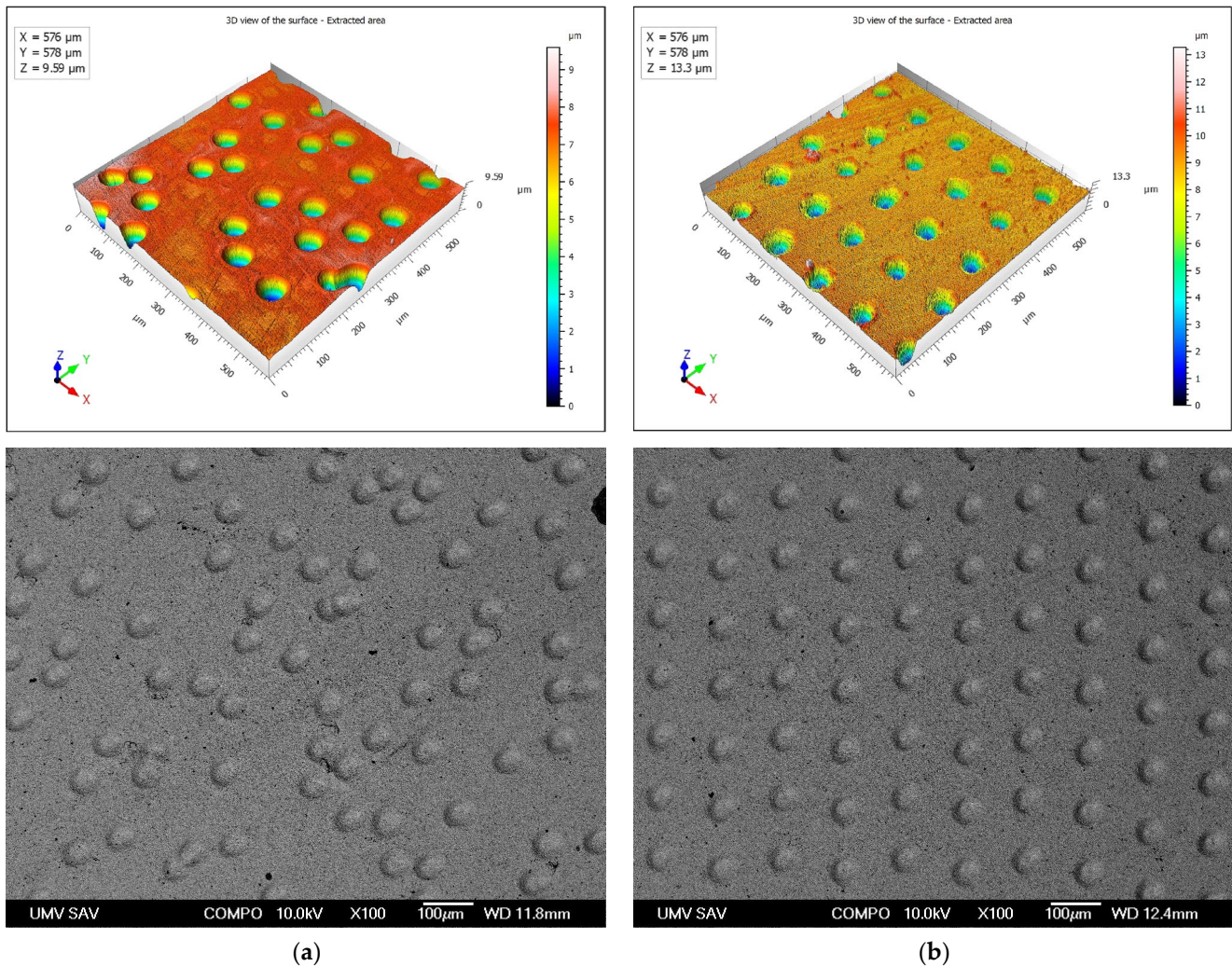
An ordered (regular) dimple texture and a stochastic dimple texture were formed on the BM surface, Figure 7. The depth of the pits was around 5 μm for both types of texture. For the surface texturing of moulds, it is recommended, due to the complex shape of mould cavities, sharp transitions, curves, and chamfers, to prefer random surface texturing rather than ordered texturing.

3.4. Tribological Properties of PVD Duplex Coatings

Table 5 shows the average COF values for the PVD duplex coatings deposited on textured and non-textured surfaces.

Table 5. The average COF values without and with laser-textured PVD duplex coatings.

COF	Duplex AlTiN G	Duplex Al ₁ N ₃	Duplex nACRo ⁴
Without texture	0.45	0.42	0.53
With texture	0.43	0.39	0.42

**Figure 7.** Appearance of texturized surfaces: (a) stochastic and (b) regular arrangement.

From Figure 8, the abrasive nature of the wear of the duplex AlTiN G coating applied to the non-textured surface is evident. In the first phase of friction, there was an interaction between the materials, with gradual changes occurring on the interfacial surface. Grooves were formed; the surface morphology changed, which was manifested by an increase in the COF from 0 to 0.52 in a very short time, which was related to micro-plastic deformation of the steel surface. Subsequently, the COF value stabilized and had a calm course throughout the test. The average COF value reached 0.45.

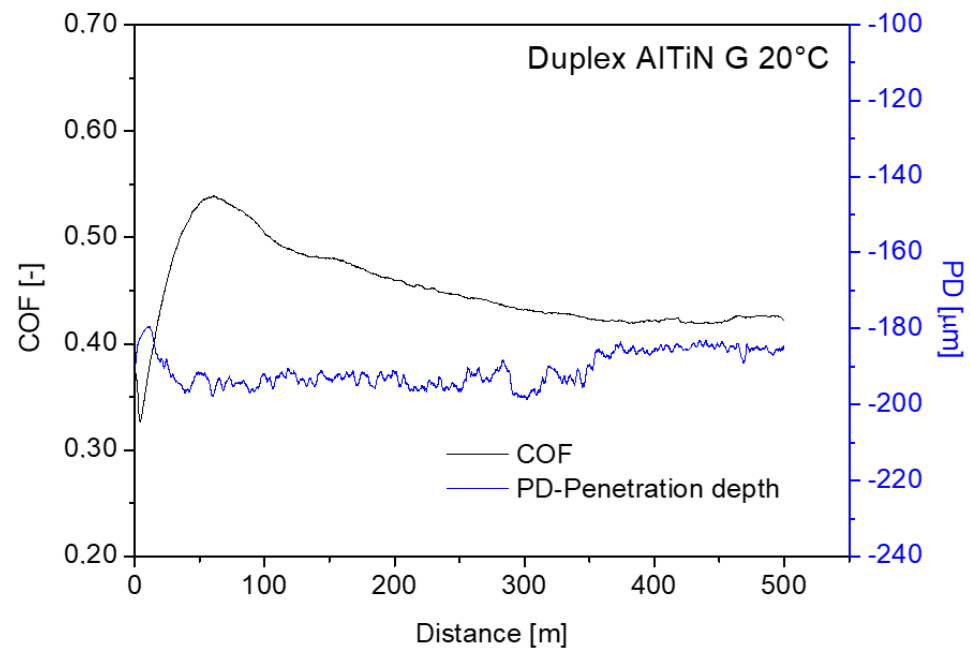


Figure 8. COF of AlTiN G coating.

When measuring the COF of the non-textured BM with a duplex AlTiN₃ coating (Figure 9) and its subsequent analysis, the abrasive character of the wear was detected together with the delamination of the coating. After passing a very short path, the COF value increased to 0.5 due to plastic deformation of the surface. After reaching the value of 0.39, the course of the COF was calm, with small fluctuations. The average value of the COF was 0.42.

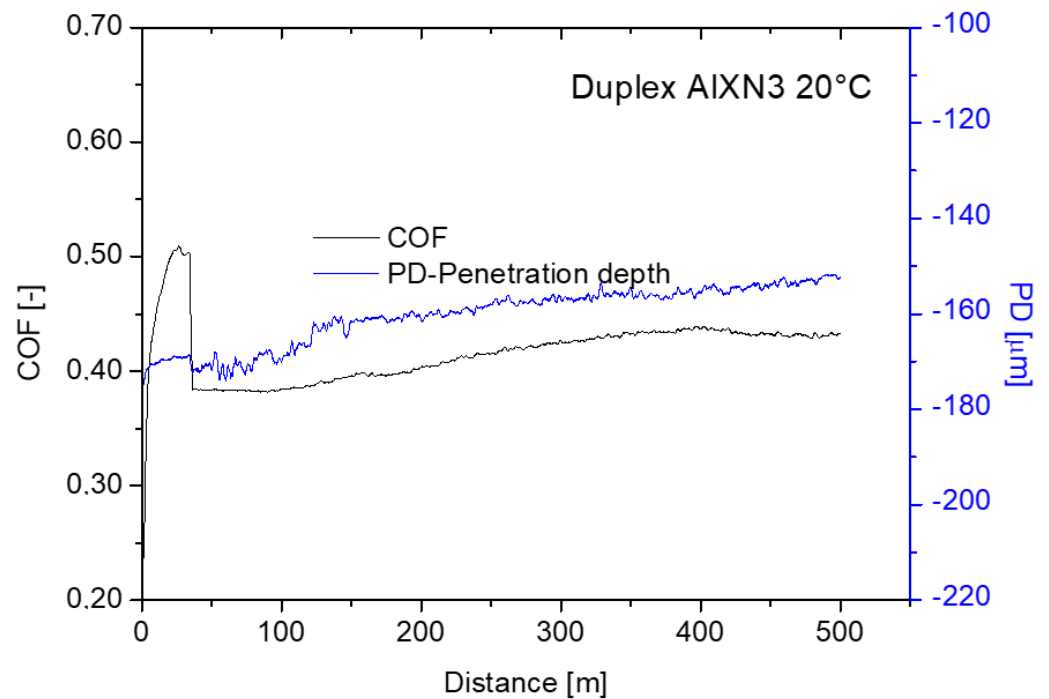


Figure 9. COF of AlTiN₃ coating.

When studying the behaviour of the nACrO₄ coating deposited on a non-textured surface (Figure 10), again, the abrasive nature of the wear was proven by the ball-on-disc test. In the first phase of contact, an interfacial area was formed, and changes gradually

occurred on this surface. These changes also resulted in an increase in the COF from 0 to 0.57 at a 50 m wear distance, which was related to micro-plastic deformation of the surface. After 200 m, a reduction in the COF (0.46) was visible where the first delamination of the coating occurred. Subsequently, after another 200 m, further delamination of the coating occurred, which led to the exposure of the underlying material. The average value of the COF was 0.53. A comparison of the COF change in the duplex PVD coatings of AlTiN G, AlXN₃, and nACRo⁴ on the non-textured substrate as a function of distance can be seen in Figure 11.

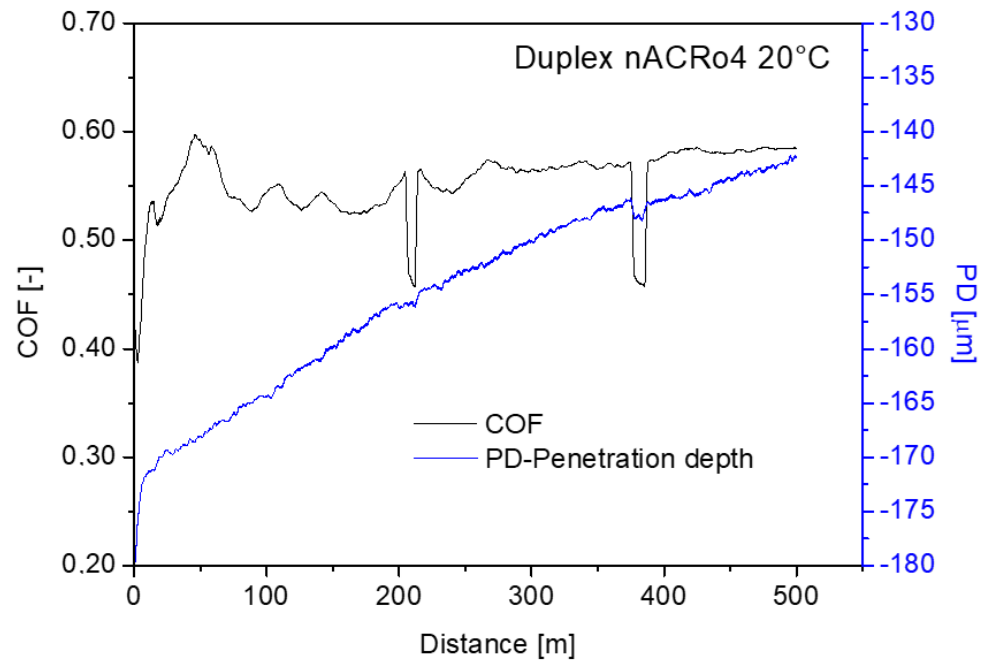


Figure 10. COF of nACRo⁴ coating.

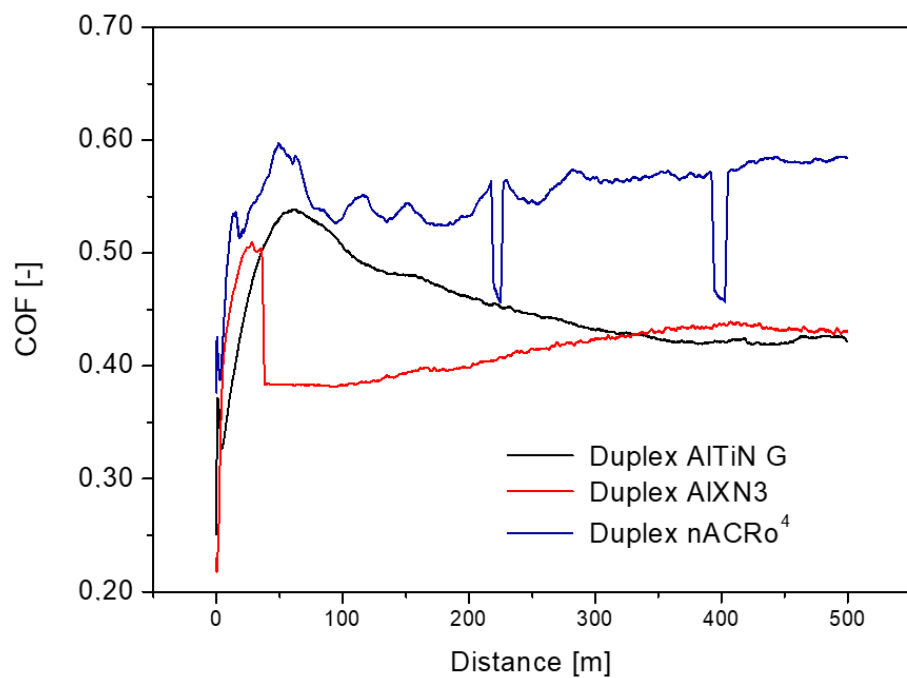


Figure 11. COF curves of duplex coatings deposited on a non-textured surface.

In the experiments on materials with a textured surface and AlTiN G coating together with stochastic well textures (LR), the measured COF values were relatively located in a narrow range of 0.38–0.44, which corresponded to an average value of 0.43 (Figure 12). Compared to the coatings deposited on the untextured surface, a reduction in the COF value due to surface texturing was identified. Friction of the material with the coating was characterized by a calm course of the COF, with a slight fluctuation in the friction force along the entire length of the friction path, with a very slight tendency to increase the value of the COF over time, except for the initial phase of the run-in. The nature of the wear during friction of the surfaces showed an abrasive behaviour. The surface along the friction track was free of the applied hard coating and was worn to a significantly lesser extent by abrasive grooving. This may have been due to the greater resistance of the surface to abrasive wear thanks to the effect of its hard coating and, later, after the removal of the hard coating through friction the laser-created micro-wells in which the hard phase of the coating process was located, which subsequently served as local hard contact surfaces that increased the service life of the surface of the samples against abrasive wear.

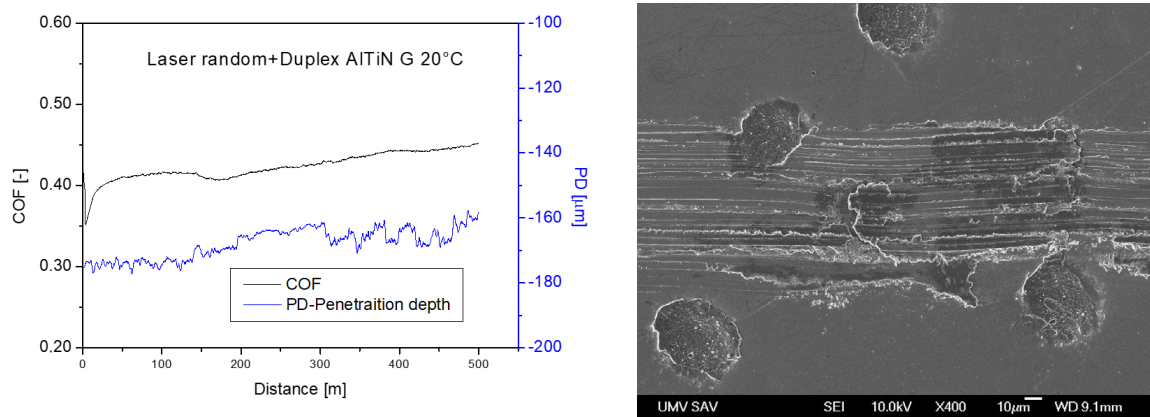


Figure 12. AlTiN G-coated surface with texture after wear.

The COF measurement of the textured surface together with the Al_xN₃ duplex coating was characterized by an initial increase in the COF value to 0.46; however, after running 100 m, the COF curve stabilized and had a calm course with minimal excursions that corresponded to an average value of 0.39 (Figure 13). Compared to the duplex coating with no textured surface, there was a reduction in the COF value due to the microtubes containing the hard phase of the coating process itself and said microtubes serving as hard contact surfaces themselves, thus increasing wear resistance. The nature of the wear was found to be abrasive.

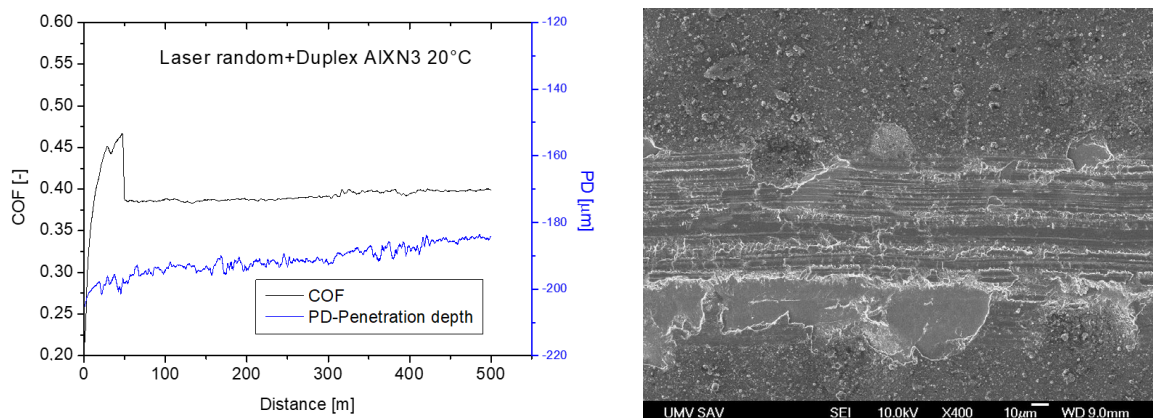


Figure 13. Al_xN₃-coated surface with texture after wear.

Abrasive wear was identified in the COF measurements of the textured surface covered with the nACRo⁴ nanostructured coating. The curve's progress during the test was gentle, with a slight excursion of the friction force along the entire friction path. The upward trend of the curve was moderate: after 300 m, the COF value ranged from 0.43 to 0.45, corresponding to an average value of 0.42 (Figure 14). Compared to the coating deposited on the untextured surface, there was again a decrease in the COF value due to the pit-like textures applied to the surface. The surface at the friction path location was equipped with a deposition-cured nanostructured coating and was worn to a significantly lesser extent by abrasive grooving. This may have been due to the greater resistance of the surface to abrasive wear thanks to the influence of the hard coating and, later, after removal of the hard coating through friction, the laser-created micro-wells containing the hard phase of the coating process, which subsequently served as local hard contact surfaces which increased the durability of the specimen surface to abrasive wear. Various authors [29–32] indicate that a combination of laser surface textures and multiple solid lubricant coatings effectively improves the tribological properties of said surfaces.

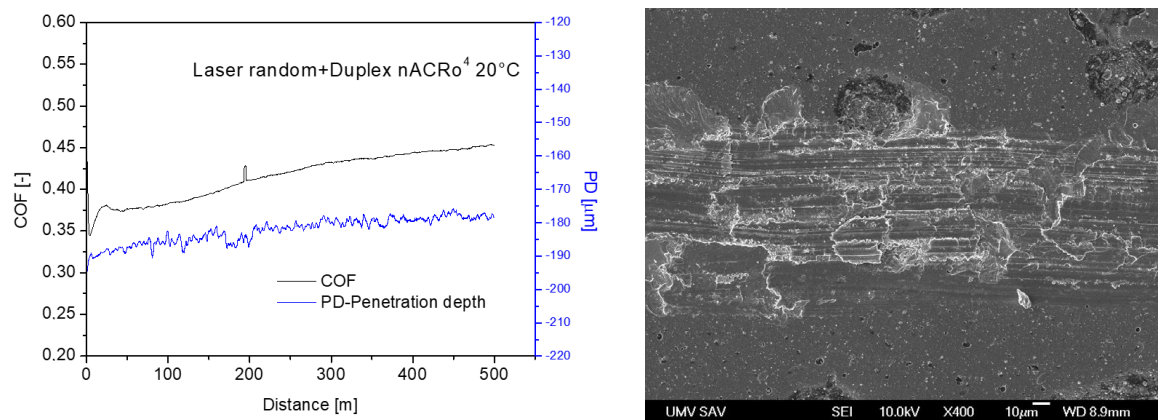


Figure 14. nACRo⁴-coated surface with texture after wear.

Figure 15 shows the COF progression of the duplex PVD coatings with applied dimple textures. The measured wear rate values of the PVD duplex coatings with laser texture are shown in Table 6. As the result of the laser-created dimples, the friction curves of the coating samples were smoother and without vibrations, and the COF's longer stable period decreased from 0.47 to 0.38 in the case of the AlXN₃ coating (Figure 15). However, a small and slowly increasing COF was obtained in the AlTiN G and nACRo⁴ samples. This shows that the laser dimple surface modifications had a good protective effect on the substrate. Similar behaviours have been observed by authors J. Chen and Z. Wu [33].

Table 6. Wear rate of textured coatings.

Coating with Texture	Wear Rate $\times 10^{-6}$ [mm ³ /m·N]
AlTiN G + LR	7.19
AlXN ₃ + LR	9.35
nACRo ⁴ + LR	0.42

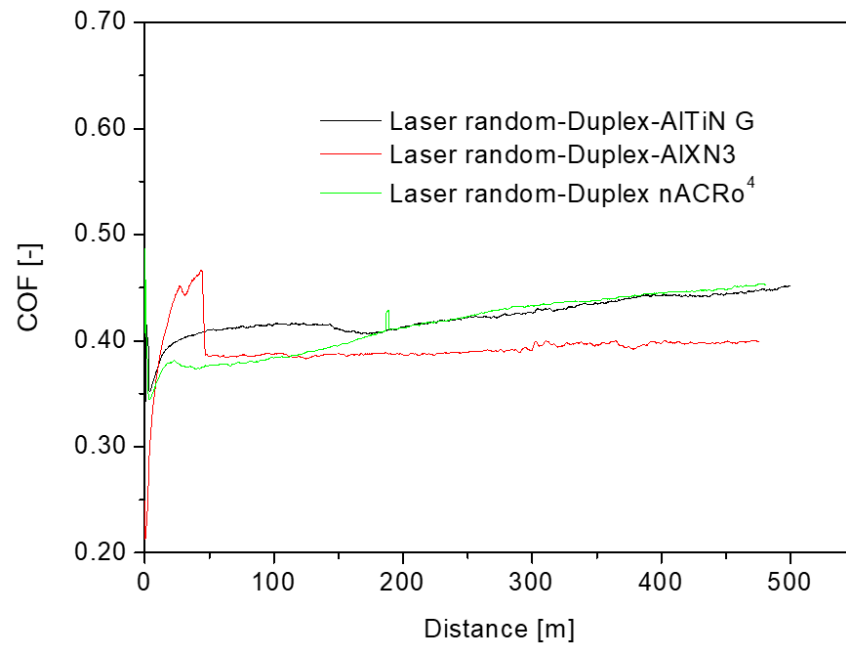


Figure 15. This COF waveforms of laser-textured duplex coatings.

The COF of the duplex PVD coatings AlTiN₃, AlXN₃, and nACRo⁴ deposited on the laser-textured surface was stable in the early stages of friction compared to the COF of the same coatings deposited on the non-textured surface (Figure 16).

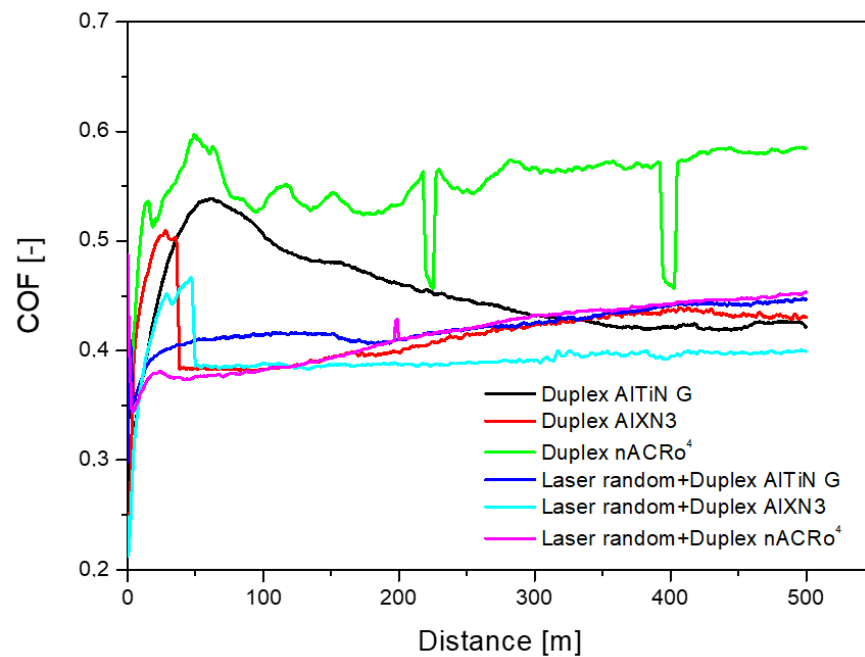


Figure 16. COF of duplex PVD coatings AlTiN₃, AlXN₃, and nACRo⁴ on laser-textured and non-textured substrates.

The high level of hardness of the ceramic coating made part of the released material adhere to the interface after ploughing using the SiC ball.

After this, the wear mechanism changed to abrasive wear and also adhesive wear caused by material transfer. As a result, the friction curves of the coating sample without laser dimples vibrated more strongly, as shown in Figure 16. This mechanism is in good agreement with Y. Chen and M. Yuan's investigation [34].

It was experimentally confirmed that the surface with a dimpled texture and applied Safety Lube 7815 separation agent exhibited lower COF values compared to the non-textured surface, and this was proven for all three PVD coatings.

4. Conclusions

The results obtained in our search for the possibility of increasing the durability of the functional surfaces of moulds for the HPDC of aluminium alloys can be summarised in the following points:

- Using visual and capillary inspection, critical areas on the mould and typical mould failures were identified: abrasive–adhesive wear, delamination of the surface layers of the material, peeling of the surface particles, and wedge-shaped branched cracks with a sharp tip at the root of the crack.
- At the points of contact with the aluminium melt, there was a discontinuous layer of separating agent and, underneath, isolated areas of surface integrity damage due to thermal fatigue and mechanical damage.
- To increase the life of the moulds, three types of duplex PVD coatings were applied to the untextured and textured surfaces of the mould's base material to reduce the coefficient of friction between the melt and the mould. Texture in the form of dimples further reduced the coefficient of friction compared to the non-textured surface. The texture was also employed to retain a small volume of mould-separating agent.
- Due to the shape complexity of the mould's cavities, it is advisable to apply stochastic dimple textures under PVD coatings.
- Using the scratch test method, it was found that the AlN₃ and nACRo⁴ coatings showed satisfactory adhesion. In the case of the duplex AlTiN G coating, coating breakage and exposure of the base material was observed.
- The depth of the pitting textures ranged between 3.5 µm and 6 µm.
- Ball-on-disc testing of the coated surfaces with a dimpled texture and Safety Lube 7815 separating agent applied confirmed a lower COF value compared to the untextured surface for all three PVD coatings.
- The lowest COF values were recorded for the nACRo⁴ coating, namely, 0.53 for the untextured surface and 0.42 for the textured surface with Safety Lube 7815 separating agent applied.
- The wear rate was lowest for the nACRo⁴ coating on the textured surface ($0.42 \times 10^{-6} \text{ mm}^3/\text{m}\cdot\text{N}$), thanks to its high hardness (40 GPa). This coating, applied to a stochastically textured surface along with the Safety Lube 7815 release agent, will ensure maximum wear reduction in exposed mould parts during the HPDC process.

Author Contributions: Conceptualization, J.B. (Janette Brezinová), M.D. and J.B. (Jakub Brezina); methodology, J.B. (Janette Brezinová), M.D. and V.P.; validation, J.B. (Jakub Brezina) and P.M.; formal analysis, J.B. (Janette Brezinová) and M.D.; investigation, J.B. (Janette Brezinová), M.D. and V.P.; resources, L.S. and M.B.; draft preparation, J.B. (Jakub Brezina), J.B. (Janette Brezinová), and M.D.; writing—review and editing, J.B. (Janette Brezinová) and A.G.; visualization, J.B. (Janette Brezinová) and M.D.; project administration, J.B. (Janette Brezinová); funding acquisition, J.B. (Jakub Brezina). All authors have read and agreed to the published version of the manuscript.

Funding: This research was funded by the Ministry of Education, Science, Research and Sport of the Slovak Republic within the project VEGA 1/0597/23: Possibilities of application of laser additive technologies in restoration of functional surfaces, KEGA 013TUKE-4/2022: Implementation of scientific research results into the processing of a modern university textbook Psychoacoustics—sound quality and acoustic design of products, as well as by the Slovak Research and Development Agency within the project APVV-20-0303: Innovative approaches to the restoration of functional surfaces by laser weld overlaying.

Data Availability Statement: The data presented in this study are available on request from the corresponding author.

Conflicts of Interest: The authors declare no conflicts of interest.

References

1. Brezinová, J.; Viňáš, J.; Guzanová, A.; Živčák, J.; Brezina, J.; Sailer, H.; Vojtko, M.; Džupon, M.; Volkov, A.; Kolařík, L.; et al. Selected Properties of Hardfacing Layers Created by PTA Technology. *Metals* **2021**, *11*, 134. [CrossRef]
2. Brezinová, J.; Džupon, M.; Viňáš, J.; Vojtko, M.; Brezina, J.; Vasková, I.; Puchý, V. Possibilities of Repairing Functional Surfaces of Molds for Injecting Al Alloys Using Manual GTAW Cladding. *Metals* **2022**, *12*, 1781. [CrossRef]
3. Zhu, Y.; Schwam, D.; Wallace, J.F.; Birceanu, S. Evaluation of soldering, washout and thermal fatigue resistance of advanced metal materials for aluminum die-casting dies. *Mater. Sci. Eng. A* **2004**, *379*, 420–431. [CrossRef]
4. Domkin, K.; Hattel, J.H.; Thorborg, J. Modeling of high temperature- and diffusion-controlled die soldering in aluminum high pressure die casting. *J. Mater. Process. Technol.* **2009**, *209*, 4051–4061. [CrossRef]
5. Šarga, P.; Brezinová, J.; Viňáš, J.; Pástor, M.; Brezina, J. Impact of Cladding Technology on Residual Stresses within the Renovation of High Pressure Die Casting Molds. *Metals* **2022**, *12*, 388. [CrossRef]
6. Neto, N.D.C.; Korenyi-Both, A.L.; Vian, C.; Midson, S.P.; Kaufman, M.J. The development of coating selection criteria to minimize die failure by soldering and erosion during aluminum high pressure die casting. *J. Mater. Process. Technol.* **2023**, *316*, 117954. [CrossRef]
7. Dadić, Z.; Živković, D.; Čatipović, N.; Marinić-Kragić, I. Influence of steel preheat temperature and molten casting alloy AlSi₉Cu₃(Fe) impact speed on wear of X38CrMoV5-1 steel in high pressure die casting conditions. *Wear* **2019**, *424–425*, 15–22. [CrossRef]
8. Bai, Z.; Wu, X. Effects of soldering and wear of die-casting die during ejection: Surface roughness and casting temperature. *Eng. Fail. Anal.* **2023**, *151*, 107383. [CrossRef]
9. Liu, M.; Sang, B.; Hao, C.; Chen, G.; Yan, J. Thermal fatigue life prediction method for die casting mold steel based on the cooling cycle. *J. Mater. Process. Technol.* **2023**, *321*, 118131. [CrossRef]
10. Malleswararao, N.D.K.; Kumar, I.N.N. Investigation of tribological behaviour of DLC coating on hypereutectic Al-Si alloys, a review. *Mater. Today Proc.* **2019**, *18*, 2581–2589. [CrossRef]
11. Neto, N.D.C.; Kloenne, Z.T.; Korenyi-Both, A.L.; Midson, S.P.; Kaufman, M.J. Influence of Al/(Al)_pCr ratio and doping effects on wear and molten aluminum attack resistance in AlCrN-based PVD coatings for lube-free aluminum die casting. *J. Mater. Res. Technol.* **2022**, *20*, 1057–1078. [CrossRef]
12. Outmani, I.; Paile, L.F.; Isselin, J.; Mansori, M.E. Effect of Si, Cu and processing parameters on Al-Si-Cu HPDC castings. *J. Mater. Process. Technol.* **2017**, *249*, 559–569. [CrossRef]
13. Gamonal-Repiso, P.; Abt, T.; Sanchez-Soto, M.; Santos-Pinto, S.; MasPOCH, M.L. Influence of topographical features on the surface appearance measurement of injection moulded components. *Polym. Test.* **2021**, *93*, 106968. [CrossRef]
14. Astana, R.; Kumar, A.; Dahotre, N. *Materials Processing and Manufacturing Science*; Elsevier: Amsterdam, The Netherlands, 2006; ISBN 978-0-7506-7716-5.
15. Laser Texturing & Wettability Modification. Available online: <http://laser4mat.webs.uvigo.es/wettability-modification> (accessed on 7 December 2022).
16. Wang, Z.; Ye, R.; Xiang, J. The performance of textured surface in friction reducing: A review. *Tribol. Int.* **2023**, *177*, 108010. [CrossRef]
17. Huang, Q.; Shi, X.; Xue, Y.; Zhang, K.; Wu, C. Recent progress on surface texturing and solid lubricants in tribology: Designs, properties, and mechanisms. *Mater. Today Commun.* **2023**, *35*, 105854. [CrossRef]
18. Chen, S.; Qian, G.; Yang, L. Precise control of surface texture on carbon film by ion etching through filter: Optimization of texture size for improving tribological behavior. *Surf. Coat. Technol.* **2019**, *362*, 105–112. [CrossRef]
19. *STN EN 13018*; Non-Destructive Testing. Visual Testing. General Principles. Slovak Office of Standards, Metrology and Testing; Bratislava, Slovakia, 2017.
20. *STN EN ISO 6507-1*; Metallic Materials—Vickers Hardness Test—Part 1: Test Method. Slovak Office of Standards, Metrology and Testing; Bratislava, Slovakia, 2018.
21. *STN EN ISO 21920-2*; Geometrical Product Specifications (GPS)—Surface Texture: Profile—Part 2: Terms, Definitions and Surface Texture Parameters. Slovak Office of Standards, Metrology and Testing; Bratislava, Slovakia, 2021.
22. *ASTM G133-05*; Standard Test Method for Linearly Reciprocating Ball-on-Flat Sliding Wear. ASTM International: West Conshohocken, PA, USA, 2016.
23. Hašul', J. Research into a New Generation of Multilayer Nanostructured PVD Coatings to Enhance Technological Lifetime of Moulds. Ph.D. Thesis, Technical University of Košice, Faculty of Mechanical Engineering, Košice, Slovakia, 2023.
24. Cadena, N.L.; Cue-Sampedro, R.; Siller, H.R.; Arizmendi-Morquecho, A.M.; Rivera-Solorio, C.I.; Di-Nardo, S. Study of PVD AlCrN Coating for Reducing Carbide Cutting Tool Deterioration in the Machining of Titanium Alloys. *Materials* **2013**, *6*, 2143–2154. [CrossRef] [PubMed]
25. Ma, D.; Liu, Y.; Deng, Q.; Li, Y.; Leng, Y. Microstructure and Mechanical Properties of TiN/Ti₂AlN Multilayers. *Coatings* **2023**, *13*, 329. [CrossRef]
26. Li, B.; Xu, Y.; Rao, G.; Wang, Q.; Zheng, J.; Zhu, R.; Chen, Y. Tribological Properties and Cutting Performance of AlTiN Coatings with Various Geometric Structures. *Coatings* **2023**, *13*, 402. [CrossRef]
27. Ramírez-Reyna, F.O.; Rodríguez-Castro, G.A.; Figueroa-López, U.; Morón, R.C.; Arzate-Vázquez, I.; Meneses-Amador, A. Effect of nitriding pretreatment on adhesion and tribological properties of AlCrN coating. *Mater. Lett.* **2021**, *284*, 128931. [CrossRef]

28. Tkachev, D.; Zhukov, I.; Nikitin, P.; Sachkov, V.; Vorozhtsov, A. Structure and Frictional Properties of Ultrahard AlMgB₁₄ Thin Coatings. *Nanomaterials* **2023**, *13*, 1589. [[CrossRef](#)]
29. Xing, Y.; Deng, J.; Wang, X.; Meng, R. Effect of laser surface textures combined with multi-solid lubricant coatings on the tribological properties of Al₂O₃/TiC ceramic. *Wear* **2015**, *342–343*, 1–12. [[CrossRef](#)]
30. Ji, M.; Zhang, H.; Xu, J.; Li, C.; Yu, D.; Chen, M.; El Mansori, M. Toward the mechanisms of surface texturing on the wear behavior of dental zirconia ceramics under dry and saliva lubricated conditions. *Wear* **2021**, *484–485*, 203845. [[CrossRef](#)]
31. Kumar, C.S.; Patel, S.K. Effect of WEDM surface texturing on Al₂O₃/TiCN composite ceramic tools in dry cutting of hardened steel. *Ceram. Int.* **2018**, *44*, 2510–2523. [[CrossRef](#)]
32. Xing, Y.; Wang, X.; Du, Z.; Zhu, Z.; Wu, Z.; Liu, L. Synergistic effect of surface textures and DLC coatings for enhancing friction and wear performances of Si₃N₄/TiC ceramic. *Ceram. Int.* **2022**, *48*, 514–524. [[CrossRef](#)]
33. Chen, J.; Wu, Z. Effect of Textured Dimples on the Tribological Behavior of WC/Co Cemented Carbide in Dry Sliding with Al₂O₃/WC Ceramic. *Micromachines* **2022**, *13*, 1269. [[CrossRef](#)]
34. Chen, Y.; Yuan, M. Effect of α -Al₂O₃ Additive on the Surface Micro-Arc Oxidation Coating of Ti6Al4V Alloy. *Nanomaterials* **2023**, *13*, 1802. [[CrossRef](#)] [[PubMed](#)]

Disclaimer/Publisher’s Note: The statements, opinions and data contained in all publications are solely those of the individual author(s) and contributor(s) and not of MDPI and/or the editor(s). MDPI and/or the editor(s) disclaim responsibility for any injury to people or property resulting from any ideas, methods, instructions or products referred to in the content.